The visual stimuli attributes instrumental for collective-motion-related decision-making in locusts

Itay Bleichman [ID][a], Peleg Shefi [ID][b], Gal A. Kaminka [ID][b] and Amir Ayali [ID][a,c,*]

[a]School of Zoology, Tel Aviv University, Tel Aviv, 6997801, Israel
[b]Department of Computer Science, Bar-Ilan University, Ramat Gan, 52900, Israel
[c]Sagol School of Neuroscience, Tel Aviv University, Tel Aviv, 6997801, Israel
*To whom correspondence should be addressed: Email: ayali@tauex.tau.ac.il
Edited By Derek Abbott

Abstract

Visual interactions play an instrumental role in collective-motion-related decision-making. However, our understanding of the various tentative mechanisms that can serve the visual-based decision-making is limited. We investigated the role that different attributes of the visual stimuli play in the collective-motion-related motor response of locust nymphs. We monitored and analyzed the behavioral responses of individual locusts tethered in a natural-like walking posture over an airflow-suspended trackball to carefully selected stimuli comprising various black rectangular shapes. The experimental findings together with a prediction model relating the level of behavioral response to the visual stimuli attributes indicate a major role of the number of objects in the visual field, and a further important effect of the object's vertical moving edges. While the object's horizontal edges can be utilized in the estimation of conspecifics' heading, the overall area or visual angle subtended by the stimuli do not seem to play any role in inducing the response. Our results offer important novel insights regarding the fundamental visual-based mechanisms underlying animal collective motion and can be useful also in swarm robotics.

Significance Statement

Visual interactions are crucial in collective-motion, yet the mechanisms underlying visual-based collective-motion-related decision-making are not well understood. This study investigated the behavioral response of marching desert locust nymphs to different attributes of swarming-related visual stimuli. We demonstrate that the number of objects is a dominant factor in locust's visual-based collective-motion-related decision-making, along with a further important effect of the size of moving-vertical edges. Moreover, the total area occluded by the visual stimuli does not significantly affect the response. The experimental results are further supported by a prediction model relating the magnitude of the behavioral response to the visual stimuli attributes. These insights are valuable for understanding animal collective motion and designing swarming robots.

Introduction

The extraction and processing of information from the environment is crucial for ecological interactions in all living organisms. However, the wealth of incoming sensory input, mostly comprising irrelevant data, constitutes a burden on the animal's nervous system and requires sophisticated strategies to enable behaviorally appropriate decision-making within relevant time constraints (1, 2). This challenge is brought to an extreme in the case of collective-motion: the highly coordinated mass-movement demonstrated by many animals, including bird flocks (3), fish schools (4), mammalian herds (5), and insect swarms (6). In all these examples, the generation and maintenance of synchronized motion is dependent on local interactions among neighboring individuals (7, 8). These interactions are, in many if not in most cases, visual (9, 10). The visual-based collective motion-related decision-making requires each agent to obtain detailed information about its neighboring conspecifics, such as estimating their relative distance, heading, and velocity (11, 12). Extracting such knowledge, however, may be hindered by the complexity of the social environment (e.g. by visual occlusions; (13, 14)). Our understanding of the fundamental mechanisms of visual information extraction and processing in such settings is poor, and is currently an area of active research (10, 15–17).

Given the limited neural resources available to the organism (18, 19), an important aspect of the various putative mechanisms that might serve visual-based decision-making is their related level of computational demands. In larval zebrafish, for example, retina-wide visual projections have been shown to be instrumental in collective motion, with the difference between the total occupancy experienced by each eye affecting the individual larva's

decision regarding turning (10). Theoretical work on flocking starlings has suggested that a similar mechanism can exchange long-range information, facilitating global interactions that maintain the density and coherence of the flock (20). Such a mechanism does not require identification or even extraction of the individual objects among the visual field. A somewhat related yet different common strategy for visual-based decision-making, which is considered "cheap" in computational demands, is based on optic-flow (21). The deformation of the image subtending the retina (the optic flow field) provides a rich source of spatial information (22). The apparent motion of objects and surfaces on the horizontal plane (translational optic flow), caused by their real motion or by the agent's self-motion, can provide information regarding their relative speed and relative distance from the agent. In many organisms, these cues are used for navigating the physical environment (23–26). In optic-flow-based decision-making, there is a very specific role for visually distinguished edges, supplying the behaviorally relevant information that is crucial in many decision-making scenarios (27–31).

An alternative, more complex or computationally demanding, approach involves object recognition, i.e. identifying the surrounding objects (e.g. conspecifics) and their specific attributes (32–34). For example, unlike their larvae, sexually mature zebrafish rely on the unique spatial attributes of their conspecific's motion for visual recognition (17).

Visual-based collective motion-related decision-making is also a key aspect in the emerging field of swarm robotics. Swarm robotics is dedicated to the development of collectively operating robots, each restricted to local perception and action but collectively displaying "swarm intelligence" in order to successfully tackle a wide range of tasks (35). In order to be as robust and flexible as their natural counterparts, collaboration between the individual robotic agents requires a decentralized individual decision-making system that will maintain synchrony and coordination (36). The visual system (i.e. computer vision) has a central role in coping with these demands (37–40), and the question of the required complexity of the visual sensors and related computer hardware on each individual robot is critical (also taking into account size, energy, and price constraints). Bio-inspired and visual-based collective-motion research is thus essential to advance the field of swarm robotics.

The desert locust, *Schistocerca gregaria* (Acrididae), is a quintessential example of a swarming organism. Its marching nymphs, forming huge devastating bands, depend on visual perception for their collective-motion-related decision-making within the complex and noisy physical, and mostly social environment (9, 41). Our previous research has shown that locust nymphs demonstrate decision-making-related responses when presented with visual stimuli comprising moving objects (computer screens showing random dot kinematograms (RDKs)—moving black discs on a white backgrounds). We established the existence of several decision rules utilized by the locusts, including a stimulus direction-dependent response, filtering by way of a speed threshold, a coherence threshold for identifying the dominant direction of the crowd, and more (41). Major questions, however, have remained unanswered. These include, for example, the question of whether locusts are sensitive to the overall area or visual angle subtended by moving objects in their visual field; or is the spatial organization of these objects the major factor affecting their response? What is the relative importance of the number of objects vs. distinct attributes of the individual objects? And more.

Here we investigated the involvement of mechanisms such as the aforementioned in visual-based swarming-related decision-making in the desert locust. Using a well-established experimental set-up (41, 42), we presented carefully controlled visual stimuli to individual locusts, monitored their behavioral responses and analyzed the effects of distinct characteristics of the visual stimuli. The specific features tested included the number of discrete objects, the (moving) vertical-edges, and the total area of the stimuli. From the perspective of the animal, these can represent the number of neighboring conspecifics, the height of the observed neighbors, and the total area occupied by them (projected onto the eye) (Fig. 1A).

To gain insights into the locust brain's inner workings and underlying computation, we further investigated the obtained behavioral data by means of a theoretical (prediction) model representing the nymph decision-making process.

Our results offer important novel insights regarding the fundamental visual-based mechanisms underlying information extraction and processing in the complex and cluttered social environment. Specifically, our findings indicate certain distinct attributes of the visual stimuli that are instrumental for collective motion-related decision-making in locusts.

Results

The experimental setup and utilized visual stimuli (Fig. 1B) were previously demonstrated to induce collective-motion-related responses from desert locusts (41, 42). In short, locusts were tethered in a natural walking posture above an airflow-suspended trackball between two parallelly placed LCD screens, positioned 15 cm from the locust on either side (circa. centered parallel to each eye). Locusts were presented with RDKs comprising randomly positioned black shapes moving over a white background. The dimensions of the presented shapes were initially set in pixels using computer software. However, in order to allow discussion in the context of visual perception terminology, they are described and referred to henceforth in millimeters (mm) or angles (subtended visual angle). For example, a 16×16-pixel lattice square equates to 4.4×4.4 mm^2 on screen (see Methods for details), corresponding to a subtended (horizontal) visual angle of 1.68°. All objects moved on both screens in parallel at 5 cm/second in a direction opposite (180°) to the tethered locust's heading (i.e. backward). As noted, each object was randomly positioned on the screen and repositioned randomly on the same screen when arriving at the edge of the screen. For further details on the rationale behind these visual parameters, see (41).

The presented stimuli comprised different combinations of the following specific attributes (Fig. 1A; and see details of the different stimuli in Table 1): (a) N denotes the number of moving objects presented; (b) S denotes the total area (mm²) covered by the objects in the entire visual field; and (c) V denotes the total moving vertical edges (mm) in the entire visual field (vertical edge—as the stimulus motion was always horizontal). Given the differing reports on the precise characteristics of locust visual acuity (43, 44), we conducted a series of preliminary experiments that identified the minimal stimulus size required to elicit a behavioral response from the locust (Fig. S1). All the parameters of the different stimuli used are described in Table 1 and illustrated in the Supplementary Video S1.

The tethered locusts' behavioral responses were characterized utilizing two major parameters: *Motion Fraction*—the fraction of time spent walking during the experiment, and *Pause Duration*—the average duration of a pausing bout (41, 42).

A behavioral visual-based swarming-related threshold

Previously reported behavioral experiments have suggested a swarming-related threshold—a certain number of marching
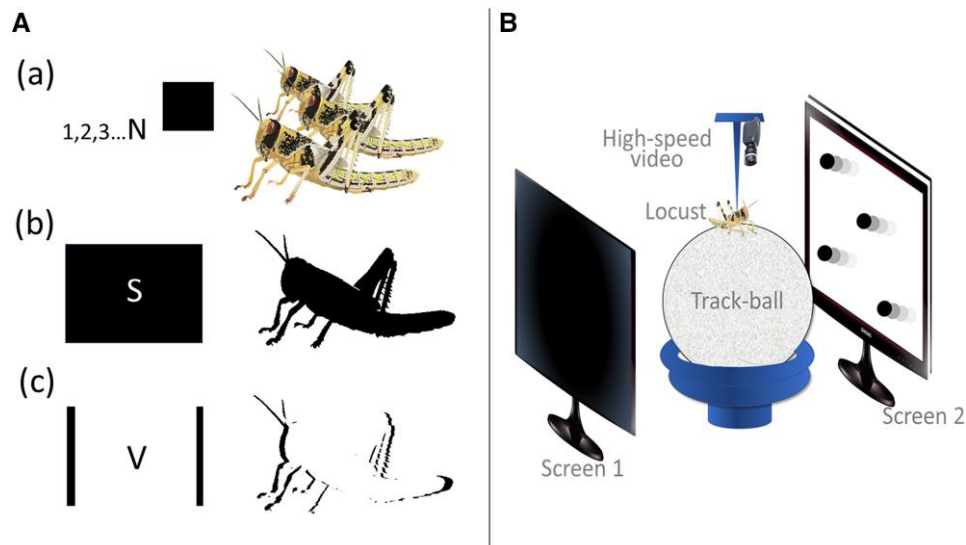
Fig. 1. A) The specific features of the visual stimulus tested. (a) Modifying the number of moving objects seen. (b) Modifying the total area or visual angle subtended by the entire visual stimulus. (c) Modifying the moving-edges (vertical edge) within the entire visual stimulus. B) Experimental setup. Each single locust was tethered in a natural-like walking posture over an airflow trackball between two LCD screens placed on both sides of the locust. Visual stimuli consisted of RDKs comprising randomly positioned black shapes over a white background, moving in a direction 180° to the tethered locust's heading. Image modified from (41).

Table 1. Properties of the different visual stimuli used in the experiments.

Stimulus	N, number of objects	Edges of one object in mm (vertical, horizontal)	Visual angles subtended by one object (vertical, horizontal)	E, Total vertical edges (mm)	S, Total area (mm²)
A	20	(4.4, 4.4)	(1.7°,1.7°)	176	387
B	10	(4.4, 4.4)	(1.7°,1.7°)	88	193
C	5	(4.4, 4.4)	(1.7°,1.7°)	44	97
D	1	(4.4, 4.4)	(1.7°,1.7°)	8.8	19
E	4	(6.9, 6.9)	(2.6°,2.6°)	36	190
F	4	(11, 4.4)	(4.2°,1.7°)	88	193
G	4	(4.4, 11)	(1.7°,4.2°)	35	193
H	1	(176,4.4)	(60°,1.7°)	352	774

conspecifics that is required to facilitate the emergence and build-up of synchronized marching (9, 45, 46). We first wanted to re-affirm these observations, and determine this behavioral threshold in our experimental setup, in order to enable further investigation of the factors involved in the swarming-related visual-based decision-making. Four different stimuli were used, comprising 20, 10, 5, or 1 similar 4.4×4.4 mm² per screen (stimuli A–D in Table 1).

The results presented in Figure 2 suggest an overall number of stimuli-dependent reduction in the motion fraction, accompanied by an increase in the pause duration. A statistically significant change in the behavioral response (both tested parameters) was observed upon reducing the number of stimuli on each screen to five or less (Fig. 2, $N = 14$–15, Kruskal–Wallis test, $P < 0.001$, Dunn's multiple comparisons test, $P < 0.05$ for both parameters). Confirming previous reports (45) these findings suggest a behavioral threshold of between 5 and 10 moving objects.

Total size of moving-edges affects swarming-related behavior

While the previous experiment confirmed the existence of a swarming-related behavioral threshold, the utilized stimuli differed in all the possible-related attributes: N denotes the number of objects, S denotes the total visual angle subtended, and V denotes the total length of vertical edges (Table 1). The following experiment was therefore aimed at determining the relative role of the total visual angle vs. the length of moving-edges in the swarming-related decision-making (S vs. V). Three different visual stimuli were used (stimuli E–G in Table 1), all comprising the same number of rectangular objects—4, with the same total area on each screen ($S = 190$–193 mm²), but with different aspect ratios and thus different edges length. The behavioral responses to these three types of stimuli were also compared with the previously observed responses towards stimulus B in Table 1 (10, 4.4 × 4.4 mm from the previous experiment) since its total area was also 193 mm².

As can be seen in Figure 3 ($N = 14$–17, Kruskal–Wallis test, $P < 0.01$, Dunn's multiple comparisons test, $P < 0.05$), reducing the number of objects on each screen from 10 to 4, with a concomitant reduction in total length of moving-edges, significantly reduced the walking fraction (stimuli II vs. I in Figure 3). However, retaining the length of moving-edges by using a rectangle with longer vertical lattice, partially recovered the walking fraction (stimuli III vs. II in Figure 3). This occurred despite the fact that the number of objects used was below the previously noted behavioral threshold. Increasing the horizontal lattices had no effect (stimulus IV vs. II in Figure 3). A similar trend (though not statistically significant) was also observed when comparing the pause duration data (i.e. a number of object-dependent changes that is reverted upon increasing the total length of moving-edges).

These findings clearly demonstrate the role of the total length of moving-edges in the locust swarming-related decision-making and suggest that the total stimulus area has little to no effect. They do not, however, reveal whether the moving edges are the dominant factor and sufficient in determining the response, or
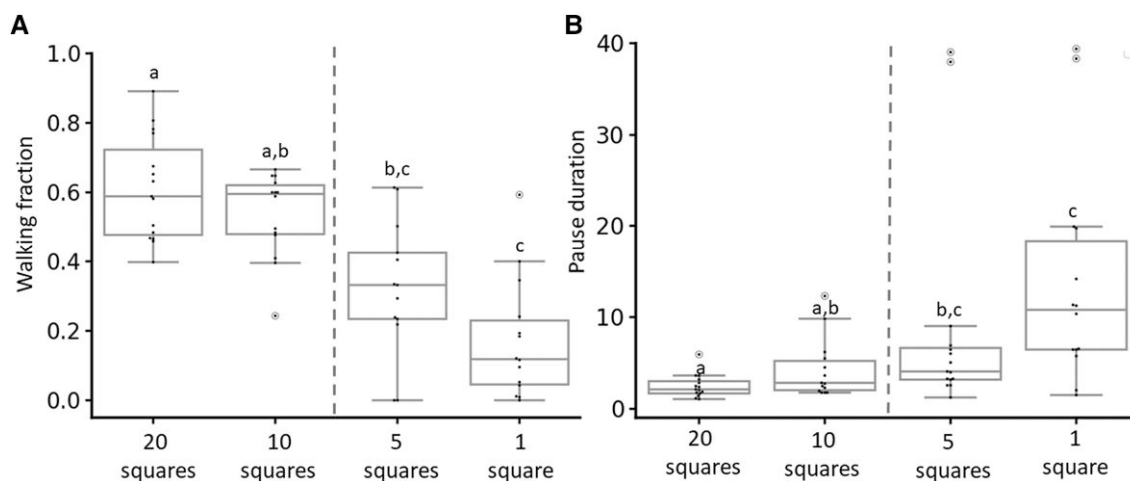
Fig. 2. A behavioral, visual-based swarming-related threshold. Walking fraction A) and average pause duration B) in response to stimuli with different numbers of objects (4.4 × 4.4 mm, 1.68°×1.68° squares). Each point represents data from a single locust (N = 14–15) Gray lines denote the median. Boxes show the interquartile range (25th to 75th percentiles). Whiskers include points up to 1.5 times the interquartile range. Significant differences are present between boxes with different letters. Gray dashed line indicates location of behavioral threshold.
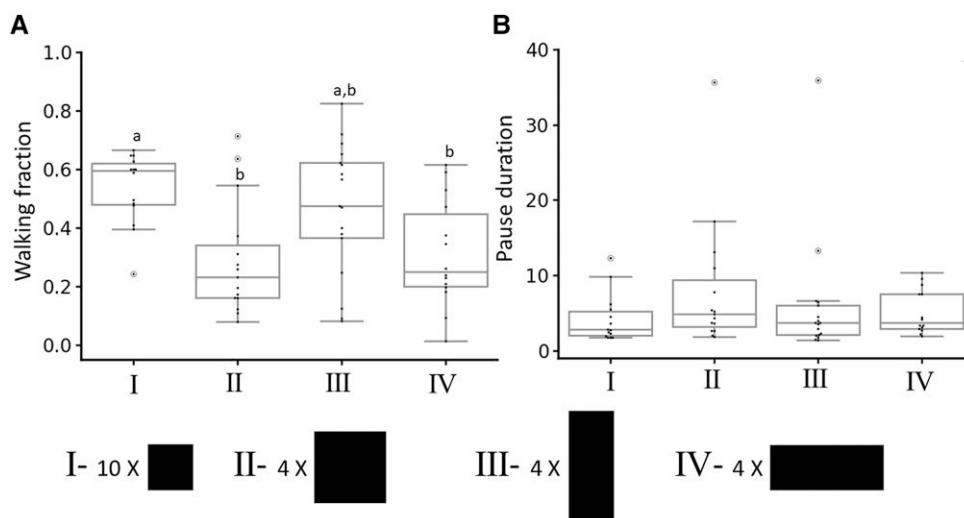

Fig. 3. The behavioral response to objects with different length of moving edges. Walking fraction A) and average pause duration B) in response to the different stimuli. The quantity and spatial properties of the different stimuli are illustrated at the bottom of the Figure. Each point represents data from a single locust (N = 14–17) Gray lines denote the median. Boxes show the interquartile range (25th to 75th percentiles). Whiskers include points up to 1.5 times the interquartile range. A) Significant differences are present between boxes with different letters. B) No significant difference between the different stimuli.

whether it is the interplay between traits that is important. This was tested in the following experiment.

Swarming-related decision-making is determined by an interplay between traits

Assuming that the moving-edge pixels are the only behaviorally relevant swarming-related visual cue, any number of objects with a total number of moving-edge pixels that is higher than the behavioral threshold should induce a prominent response. We tested this assumption in an "extreme" scenario, presenting a stimulus composed of one long vertical bar, with 176 × 4.4 mm lattices (stimulus H in Table 1), and compared the behavioral response it generated to that demonstrated towards a stimulus comprising 20, 4.4 × 4.4 mm^2, randomly distributed across the screen (stimulus A in Table 1), which is an above-threshold stimulus that was shown to induce an increased walking fraction and

decreased pause duration. The single long bar comprised a total length of 352 mm of moving-edges compared to only 176 mm in the multiple squares stimulus.

As presented in Figure 4, despite this extremely high length of moving-edges, the single-bar stimulus induced responses characterized by a significantly lower walking fraction and a significantly higher pause duration compared to the 20 square stimulus (Fig. 4, N = 13–15, Mann–Whitney test, P < 0.05 for both parameters). The results of this final behavioral experiment indicate that an interplay exists between the visual attributes tested, in particular between the number of objects and the moving-edge pixels.

A model predicting the level of behavioral response to the visual stimulus attributes

We attempt to develop a predictive model relating features of the visual stimuli to the swarming response. The controlled visual
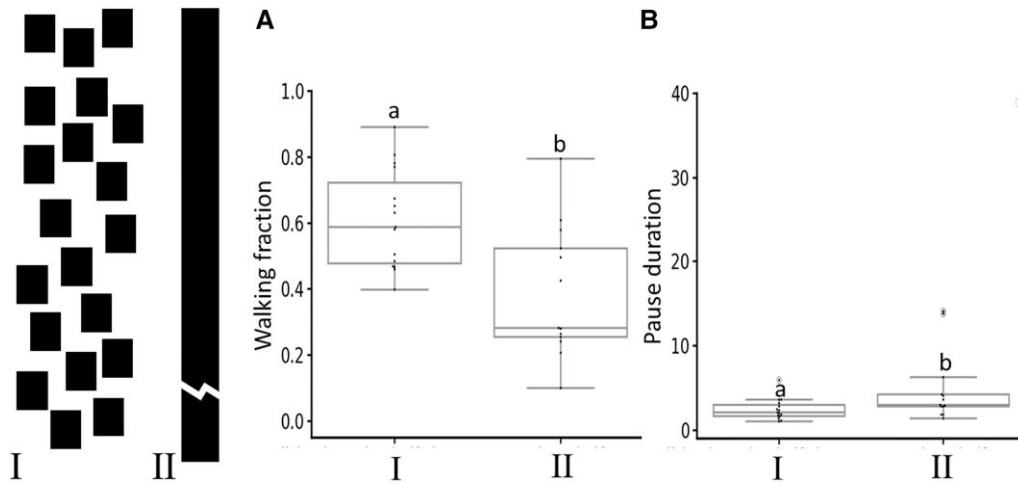
Fig. 4. Swarming-related behavioral response is determined by an interplay between the number of objects and the length of moving-edges. Walking fraction A) and average pause duration B) in response to the different stimuli. Each locust was presented with either: I—twenty 4.4 × 4.4 mm², *randomly dispersed* over each screen (the arrangement of the squares in the figure is for demonstrating their number only), or II—a long bar. Each point represents data from a single locust ($N = 13$–15). Gray lines denote the median. Boxes show the interquartile range (25th to 75th percentiles). Whiskers include points up to 1.5 times the interquartile range. Significant differences are present between boxes with different letters.

stimulus' features comprised the number of objects presented (N), the size of the vertical edge (V) (i.e. the observed object's height), and the horizontal edge (H) (i.e. its horizontal width projection).

First, for each neighbor, the model relies on an assumption that the response of the locust is heavily dependent on the distance to the observed neighbor, and the neighbor's heading relative to the locust. These two measurements are utilized in most common collective motion algorithmic models (6, 14). The subtended angles of the vertical edge and the horizontal edge of an object on the locust's compound eye serve, under some assumptions, as proxies to these measurements (Fig. 5).

Distance (range) to neighbor

As pointed out in (14), the subtended angle of the horizontal edge can serve as a proxy for the distance, but is highly noisy, since it varies greatly depending on the orientation of the neighbor with respect to the observer. However, the vertical edge is far less noisy for neighbors at eye's level (on the ground). Figure 5 shows an idealized angle subtended on the vertical edge V. The distance R is the length of the line segment cutting the angle in half (α), and forming a 90° angle with V. Under the assumption that the locust knows—even implicitly—the typical size of its conspecifics, and practically their expected vertical height V, it could compute R in units of its own body-measurements (Eq. 1). Practically, this means the angle α may be a key component in the locust's decision-making.

$$R = \frac{V/2}{\tan(\alpha)} \quad \Rightarrow \quad \alpha = \arctan\left(\frac{V}{2R}\right) \tag{1}$$

Relative heading of neighbor

Once the distance is known to the locust, the relative heading of the neighbor can be estimated fairly reliably as well. We examine the *horizontal* right triangle (parallel to the ground plane), formed by the angle β subtended on half of the horizontal edge H, and the edge of length R, which is assumed to be perpendicular to the horizontal edge H. In this triangle, we are interested in the angle Ψ (Eq.

2), since it can be used, together with the neighbor's bearing angle, to compute the relative heading of the neighbor.

$$\Psi = \arctan\left(\frac{2R}{H}\right). \tag{2}$$

The predictive model we present ties these components together (Eq. 3). We assume that the locust evaluates each visually perceived object separately using the above geometric reasoning. It then responds to the aggregated evaluations as described below. The relationship between the two visual angle components (Eq. 1, 2) is nonlinear, and their hypothetical use in the locust undoubtedly involves additional factors. Nevertheless, we chose a simplified-rudimentary model, based on these basic components only. Thus, the values for the two angles are simply multiplied to account for nonlinearity, and the distance R (which somewhat varies as the object moves in a parallel trajectory to the focal locust) is not included. As the locust is visually tracking N objects, we hypothesize that its level of response will follow a logarithmic curve, based on Weber–Fechner Law (47). Putting all these factors together (following Eqs. 1 and 2), yields Eq. 3.

$$F(V, H, N) = \log\left[N \arctan\left(\frac{V}{2}\right) \arctan\left(\frac{2}{H}\right)\right], \tag{3}$$

where F being the focal locust's predicted response level. As noted, the model is incomplete; we neither avoided conjecturing on the role of additional factors that influence the locust decision-making, nor does the model include all behavioral measures used in the experiments (i.e. walking faction, pause duration). As shown below, however, it further validates our experimental observations regarding the role and significance of distinct properties of the visual stimuli, as it is successful in linking the observed behavior to the different stimuli presented.

The model prediction is correlated with the experimental results

Following (48), we plot the model predictions (horizontal axis, marked F), against the observed experimental response, as measured by the *mean* walking fraction in each experimental setting, on the vertical axis (Fig. 6). The bars mark the standard error

$$\Psi = arctan\left(\frac{2R}{H}\right) \qquad\qquad R = \frac{V/2}{tan(\alpha)}$$
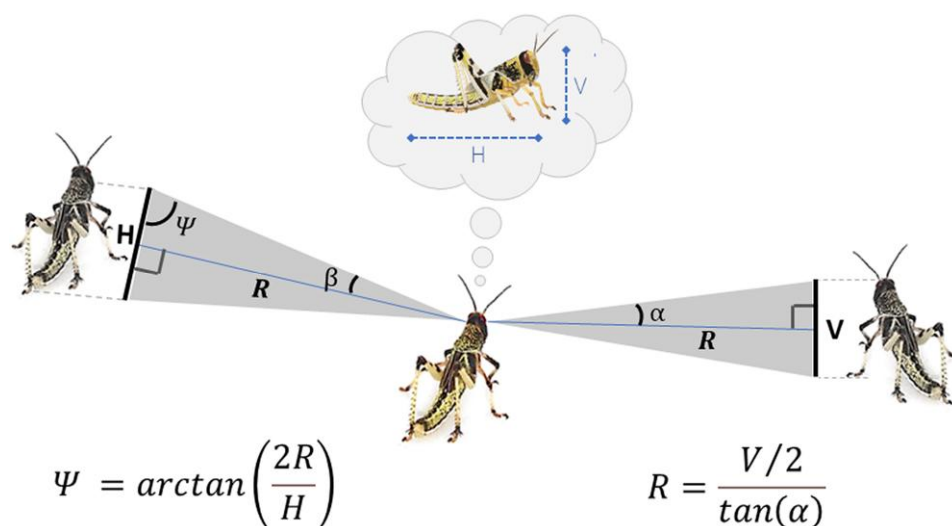
Fig. 5. Utilizing visual stimuli and an estimated notion of the size of a locust in order to infer distance and direction of neighboring locusts in the swarm. The focal locust (center) can deduce the distance (R) to a neighbor in the swarm based on the expected vertical edge (V) and the subtended angle of half the vertical edge (α). The distance from the focal locust (R) together with the subtended horizontal angle (β) and the expected horizontal edge (H) can serve to compute the angle Ψ, which plays a role in estimating the relative heading of conspecifics in the swarm.
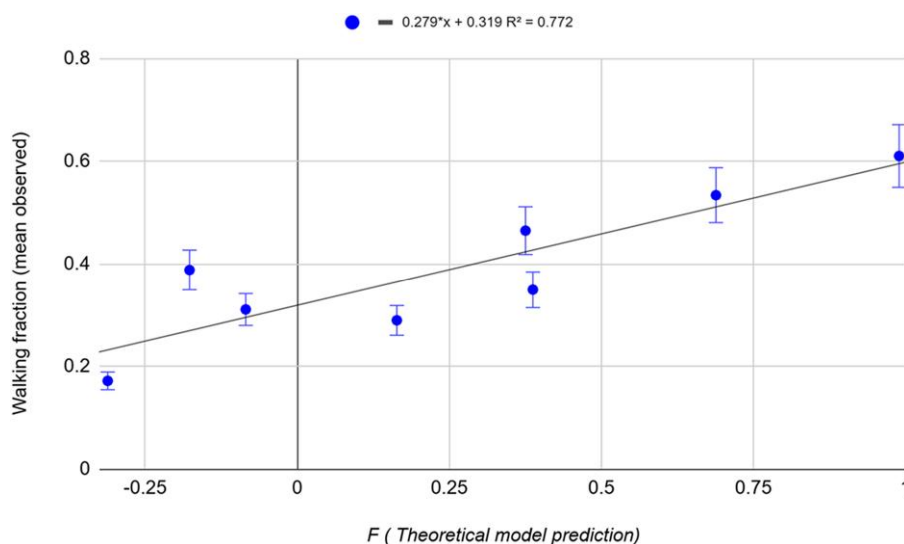

Fig. 6. Model predictions and correlation with the locusts' behavioral response. The predicted response (Eq. 3) is measured on the horizontal axis. Dots depict the associated mean walking fraction observed for the experimental groups (stimuli A–H in Table 1). The solid line shows the linear regression (R^2 =0.772, *Eq: WF Response* = 0.121F + 0.319). Error bars denote the standard error of the mean.

around the arithmetic mean (commonly called the average) of the observed data (see Supplementary Material for a discussion of why the geometric mean may also be appropriate, and Fig. S2 for the prediction model using the geometric mean).

The linear regression shown in the figure allows assessment of the model's prediction compared with the observed mean walking fraction. Its relatively high R^2 score indicates a good fit: i.e. the model is a good predictor of the response to the controlled visual stimuli. Ideally, if it had accounted for all the variance among individual locusts and the different trials, all dots would fall exactly on the line. We show the residual plot in Fig. S3. Also, as the model is rudimentary, it does not directly predict absolute walking fraction values, thus its intercept and slope angle are not 0° and 45°, respectively.

Discussion

In order to successfully negotiate their surroundings and move in the environment, organisms make repeated sensory-information-based decisions. These are highly dependent on both the intricacy of the environment, and the complexity of the movement-related behavioral task (49, 50). Collective motion presents an exceptionally demanding task within a very complex environment: Collective-motion-related decision-making requires the processing of ample information regarding the physical and social surroundings of the organism (41). Each organism repeatedly takes decisions to ensure that its route is collision free, while also maintaining the ordered motion of the swarm within the highly cluttered and noisy surroundings.

In the case of visual-based collective motion, decision-making is particularly challenging due to constraints on the visual field, the need to filter nonrelevant information, and the computational burden of extracting of relative speed and relative heading of conspecifics. These are just as crucial for collectively moving living organisms as they are for swarming robots (14–16, 37, 51–53). Several theoretical mathematically formulated biomimetic approaches have been shown to cope successfully with these difficulties, such as optic-flow-based navigation (15) and visual projection (20). However, the question of the mechanisms used in nature, by moving animals (birds, fish, insects), remains largely open.

Here we investigated this question in desert locust nymphs. Focusing on the relative roles of different attributes of the visual stimuli in generating swarming-related behavioral responses, we provide insights into the visual-based collective-motion-related decision making. We directly tested the possibility of the locusts relying only on basic changes over time in their visual field (e.g. optic flow), compared to the more complex alternative: utilizing the recognition of the number of moving objects in the visual field. Previous arena swarming experiments have already suggested that the walking kinematics of locusts is strongly dependent on the number of surrounding moving objects, with a clear threshold (9, 45, 54). The distinct behavioral responses in such experiments, however, could depend on the different attributes of the visual stimuli that change concomitantly with the number of objects, including the overall area subtended in the individual's eye and the total length of moving-edges.

To the best of our knowledge, this study is the first to directly demonstrate, at the individual animal level, the relative roles of different attributes of the visual stimuli in generating the swarming-related behavioral response. Our findings demonstrate that out of the three possible features tested, the number of objects (N) seems to play the most central role in the nymph's decision-making regarding marching. Reducing the number of objects to below the behavioral threshold significantly reduces walking fraction and increases pause duration, even when the total area subtended on the locust's eye (S) remains constant. The moving vertical edges (V), although clearly affecting the locust behavioral response, were not sufficient to maintain the level of response when the number of objects was very low.

The quantity of visual elements can be perceived by changes in various nonnumerical continuous physical variables. Different approaches have suggested continuous variables that may contribute to the evaluation of "numerousness' (55, 56). In this work, we did not address all such variables, but rather focused on those previously shown to be involved in visual-based collective-motion-related decision-making (10, 17) and insect navigation (57). The aforementioned approaches for the evaluation of the perception of numerousness will serve as a foundation for our future investigation into the role of this aspect of the locust perception in collective motion.

The presented (skeletal) prediction model facilitates predictions regarding the level of the observed behavioral responses (as measured by the walking fraction) based on the number of objects, and the visual angles subtended by the vertical and horizontal edges of the objects. It therefore provides indication of their role in locust decision-making. Interestingly, the horizontal edge pixels, in our experiments did not seem to directly affect the locust's response, are used by the model to contribute to the overall accuracy of the prediction (i.e. ignoring the perceived width leads to reduced fit; Fig. S4). The components of the model are intuitively appealing. The two angles stem directly from the geometry of the observed neighbor with respect to the observing animal, and the logarithmic relation to the number of observed neighbors follows a familiar perceptual law (47). However, the relationship between the geometric components is abstractly modeled (multiplication). More investigations are needed to flesh out the details of this relationship.

We also note that for one of the experimental groups we used a stimulus comprising a single object that is 176 mm in height, approximately six times the height of the locust. Such objects may elicit a motion response that is not social-related (58, 59). When the data for this group are removed, the model fit as measured by R^2 improves from 0.772 to 0.907 (see Fig. S5). This is an encouraging result, yet it also compounds further studies, since it implies that there is a need to further take into account interactions between social (in the gregarious, swarming sense) and other mechanisms in the locust brain that together translate visual stimuli to action.

Optic flow has previously been shown to be instrumental in various motion-related behaviors in insects, including flight control and navigation (22, 57). Our findings, however, are inconsistent with reliance on the optical flow field by itself as the dominant factor in shaping collective-motion-related decision-making. Instead, we believe that the swarming-related behavioral response is the result of an interplay between several salient properties of the visual stimuli, including the number of objects and the moving-edges (horizontal and vertical). These may be inferred or generated (by further processing) from the optical flow field. Our data are consistent with distinct roles of the moving-edges in deciphering the distance to and direction of neighboring conspecifics (14), together with a more general effect of the number of conspecifics in the visual field on the magnitude of the swarming response (i.e. affecting the collective-motion-state of the insect (60)). Accumulating evidence for visual object recognition abilities (61–66), and numerical abilities ((61, 67–70) and see (71) for a review) in various invertebrates support such a conjecture.

Our findings serve as a basis for understanding the inner workings of the individual locust when performing collective motion. By understanding the importance of the different aspects of the visual input, a more accurate mechanistic model of collective motion may be reached. Such a model can be valuable in the field of collective robotics. Further work is required in order to elucidate how collectively moving organisms define, identify (and possibly count) agents or conspecifics, including elucidating the neurophysiological mechanisms underlying all these abilities.

Methods

Animals

All experiments were carried out using Vth-instar larvae of *S. gregaria* (Forskål), taken from our high-density, gregarious-phase locust laboratory-colony at the School of Zoology, Tel Aviv University. The locusts were reared for many consecutive generations under crowded conditions with 100 to 160 individuals in 60-L aluminum cages and under a controlled temperature of 30 °C, 35 to 60% humidity, and a 12-h dark/12-h light cycle. The locusts were fed daily with wheat seedlings and dry oats.

Experimental setup

Experiments were conducted in a temperature-controlled (28 °C) and LED illuminated chamber. Individual locusts were tethered with a fixed heading using a 1 cm clear vinyl tube attached to their

pronotum, and maintained in a natural-like walking posture above an airflow-suspended Styrofoam trackball decorated with an irregular black over white pattern. Visual stimuli were presented on two parallel LCD monitors (LG, 24gn600, South Korea, 24″, 144 Hz refresh rate and a resolution of 1,920 × 1,080 pixels; Pixel size 0.2745 × 0.2745) positioned 150 mm away from the locust and perpendicular to its short axis, with the animal's eyes aligned with the center of both screens in azimuth. The locust was positioned 65 mm higher than the bottom of the screens. Each screen subtended a vertical angle of 94.4° and a horizontal angle of 122° in the locust's field of view. The tethered locust's behavior was recorded using a Sony FDR-AXP35 digital camera at a 25-fps rate.

Visual stimulation

Visual stimuli were designed using Python version 3.9.2 (Python Software Foundation) with the PsychoPy library version 2022.2.4 (72). The basic stimulus with different properties was implemented in an RDK setting, using the PsychoPy.Visual.dotstim protocol: i.e. a moving object appears at random on the screen and when reaching the edge of the screen is replaced by a new one (appearing again at a random place on the screen). The stimuli comprised black rectangles (psychoPy.visual.rect) on a white screen background. In accordance with (41), the stimuli's motion was 100% coherent—i.e. all objects moved in the same direction, 180° to the tethered locust's heading (i.e. backwards) and with a constant speed of 5 cm/s. Each experiment comprised an initial 2-min adjustment period, during which both screens were first totally black for 60 s and then totally white for 60 s. This was followed by 40 s of stimuli presentation, after which a new locust was tethered to the trackball, etc.

We comparatively examined the effects of three different features of the visual stimulus (visual parameters) on swarming-related decision-making (Fig. 1):

(a) N denotes the number of objects presented on each screen.
(b) S denotes the total area occupied by stimuli (i.e. black colored) on each screen.
(c) V denotes the total length of moving-edges—the overall length of pixels that change from black to white, or vice versa, from frame to frame during movement of all stimuli on each screen. Since the motion direction in our experimental scheme was always on the horizontal plane (backwards), V comprises the vertical lattices of the rectangular shapes utilized.

For example, the specific visual parameters for an RDK composed of five squares, each 4.4 mm by 4.4 mm in size, will be: (a) N, number of objects 5; (b) S, total area—97 mm²; and (c) V, 44 mm total length of vertical edges ((4.4*2) *5).

We conducted three different behavioral experiments, utilizing different combinations of the above visual parameters to investigate the tethered locusts' behavioral responses and the relative importance of the different parameters, as detailed in Table 1 and in the Results section. An example of the visual stimulation is available in the Supplementary Material, video.

Behavioral analysis

The tethered locusts' behavioral responses to the visual stimuli were measured utilizing *Motion Fraction*—the fraction of time spent walking during the experiment, and *Pause Duration*—the average duration of a pausing bout. The recorded experimental videos were analyzed using FicTrac (73). The trackball rotation during each frame was captured and the behavioral state of the tethered locust (motion or pause) was determined using a predetermined threshold (41) which was re-validated here. Because locust motion is intermittent (pause and go; (9, 74)), walking and pausing bouts were identified. Ten or more consecutive motion frames were considered a walking bout; and 20 or more consecutive pause frames were considered a pausing bout (similar to the thresholds used in (9, 41, 42)).

Data analysis

All the data were plotted using the Matplotlib Python package and statistical tests were performed using GraphPad Prism 10 (GraphPad Software, San Diego, CA, USA). P-values of 0.05 were deemed statistically significant.

Supplementary Material

Supplementary material is available at *PNAS Nexus* online.

Author Contributions

A.A. and I.B. designed the study. I.B. performed the experiments. I.B., P.S., and G.A.K. analyzed the data. P.S and G.A.K. constructed the model. A.A., I.B., P.S., and G.A.K. wrote the manuscript.

Data Availability

All additional data related to this paper is available in the supplementary material.

References

1 Hein AM. 2022. Ecological decision-making: from circuit elements to emerging principles. *Curr Opin Neurobiol*. 74:102551.
2 Lemasson BH, Anderson JJ, Goodwin RA. 2009. Collective motion in animal groups from a neurobiological perspective: the adaptive benefits of dynamic sensory loads and selective attention. *J Theor Biol*. 261(4):501–510.
3 Ballerini M, *et al*. 2008. Empirical investigation of starling flocks: a benchmark study in collective animal behaviour. *Anim Behav*. 76(1):201–215.
4 Miller N, Gerlai R. 2012. From schooling to shoaling: patterns of collective motion in zebrafish (Danio rerio). *PLoS One*. 7(11): e48865.
5 Ginelli F, *et al*. 2015. Intermittent collective dynamics emerge from conflicting imperatives in sheep herds. *Proc Natl Acad Sci U S A*. 112(41):12729–12734.
6 Ariel G, Ayali A. 2015. Locust collective motion and its modeling. *PLoS Comput Biol*. 11(12):e1004522.

7   Petit O, Bon R. 2010. Decision-making processes: the case of collective movements. *Behav Processes.* 84(3):635–647.

8   Gueron S, Levin SA, Rubenstein DI. 1996. The dynamics of herds: from individuals to aggregations. *J Theor Biol.* 182(1):85–98.

9   Ariel G, Ophir Y, Levi S, Ben-Jacob E, Ayali A. 2014. Individual pause-and-go motion is instrumental to the formation and maintenance of swarms of marching locust nymphs. *PLoS One.* 9(7):e101636.

10 Harpaz R, Nguyen MN, Bahl A, Engert F. 2021. Precise visuomotor transformations underlying collective behavior in larval zebrafish. *Nat Commun.* 12(1):6578.

11 Vicsek T, Czirók A, Ben-Jacob E, Cohen I, Shochet O. 1995. Novel type of phase transition in a system of self-driven particles. *Phys Rev Lett.* 75(6):1226–1229.

12 Pita D, Collignon B, Halloy J, Fernández-Juricic E. 2016. Collective behaviour in vertebrates: a sensory perspective. *R Soc Open Sci.* 3(11):160377.

13 Kunz H, Hemelrijk CK. 2012. Simulations of the social organization of large schools of fish whose perception is obstructed. *Appl Anim Behav Sci.* 138(3–4):142–151.

14 Krongauz DL, Ayali A, Kaminka GA. 2024. Vision-based collective motion: a locust-inspired reductionist model. *PLoS Comput Biol.* 20(1):e1011796.

15 Castro D, Ruffier F, Eloy C. 2024. Modeling collective behaviors from optic flow and retinal cues. *Phys Rev Res.* 6(2):023016.

16 Zampetaki A, Yang Y, Löwen H, Royall CP. 2024. Dynamical order and many-body correlations in zebrafish show that three is a crowd. *Nat Commun.* 15(1):2591.

17 Kappel JM, et al. 2022. Visual recognition of social signals by a tectothalamic neural circuit. *Nature.* 608(7921):146–152.

18 Bernays EA, Wcislo WT. 1994. Sensory capabilities, information processing, and resource specialization. *Q Rev Biol.* 69(2):187–204.

19 Warrant EJ. 2016. Sensory matched filters. *Curr Biol.* 26(20): R976–R980.

20 Pearce DJG, Miller AM, Rowlands G, Turner MS. 2014. Role of projection in the control of bird flocks. *Proc Natl Acad Sci U S A.* 111(29):10422–10426.

21 Buxton BF, Buxton H. 1984. Computation of optic flow from the motion of edge features in image sequences. *Image Vis Comput.* 2(2):59–75.

22 Egelhaaf M. 2023. Optic flow based spatial vision in insects. *J Comp Physiol A Neuroethol Sens Neural Behav Physiol.* 209(4): 541–561.

23 Srinivasan MV, Gregory RL. 1992. How bees exploit optic flow: behavioural experiments and neural models [and discussion]. *Philos Trans R Soc B: Biol Sci.* 337(1281):253–259.

24 Karlsson C, Willis J, Patel M, de Perera TB. 2022. Visual odometry of Rhinecanthus aculeatus depends on the visual density of the environment. *Commun Biol.* 5(1):1045.

25 Gläser N, et al. 2014. Harbor seals (*Phoca vitulina*) can perceive optic flow under water. *PLoS One.* 9(7):e103555.

26 Sibeaux A, Karlsson C, Newport C, Burt de Perera T. 2022. Distance estimation in the goldfish (*Carassius auratus*). *Proc Biol Sci.* 289(1984):20221220.

27 Nordström K, Barnett PD, O'Carroll DC. 2006. Insect detection of small targets moving in visual clutter. *PLoS Biol.* 4(3):e54.

28 Zeng Y, Lin Y, Abundo A, Dudley R. 2015. Visual ecology of directed aerial descent in first-instar nymphs of the stick insect *Extatosoma tiaratum. J Exp Biol.* 218(Pt 14):):2305–2314.

29 Pratt SC, Brooks SE, Franks NR. 2001. The use of edges in visual navigation by the ant *Leptothorax albipennis. Ethology.* 107(12): 1125–1136.

30 Horridge GA. 1986. A theory of insect vision: velocity parallax. *Proc R Soc Lond B Biol Sci.* 229(1254):13–27.

31 Horridge A. 2009. What does an insect see? *J Exp Biol.* 212(17): 2721–2729.

32 Peirce JW. 2015. Understanding mid-level representations in visual processing. *J Vis.* 15(7):5.

33 DiCarlo JJ, Zoccolan D, Rust NC. 2012. How does the brain solve visual object recognition? *Neuron.* 73(3):415–434.

34 Logothetis NK, Sheinberg DL. 1996. Visual object recognition. *Annu Rev Neurosci.* 19:577–621.

35 Barca JC, Sekercioglu YA. 2013. Swarm robotics reviewed. *Robotica.* 31(3):345–359.

36 Lumelsky VJ, Harinarayan KR. 1997. Decentralized motion planning for multiple mobile robots: the cocktail party model. *Autonomous Robots.* 4(1):121–135

37 Ayali A, Kaminka GA. 2023. The hybrid bio-robotic swarm as a powerful tool for collective motion research: a perspective. *Front Neurorobotics.* 17:1215085.

38 Qi J, Bai L, Wei Y, Zhang H, Xiao Y. 2023. Emergence of adaptation of collective behavior based on visual perception. *IEEE Internet Things J.* 10(12):10368–10384.

39 Weinstein A, Cho A, Loianno G, Kumar V. 2018. Visual inertial odometry swarm: an autonomous swarm of vision-based quadrotors. *IEEE Robot Autom Lett.* 3(3):1801–1807.

40 Capodieci N, Cabri G, Collaboration in swarm robotics: a visual communication approach. 2013 International Conference on Collaboration Technologies and Systems (CTS); San Diego, CA, USA. IEEE; 2013. p. 195–202.

41 Bleichman I, Yadav P, Ayali A. 2023. Visual processing and collective motion-related decision-making in desert locusts. *Proc Biol Sci.* 290(1991):20221862.

42 Aidan Y, Bleichman I, Ayali A. 2024. Pausing to swarm: locust intermittent motion is instrumental for swarming-related visual processing. *Biol Lett.* 20(2):20230468.

43 Horridge G. 1966. The retina of the locust. In: Bernhard CG, editor. *Symposium on the Compound Eye.* Pergamon Press, p. 513–541.

44 Catton WT. 1999. The effect of target orientation on the visual acuity and the spatial frequency response of the locust eye. *J Insect Physiol.* 45(2):191–200.

45 Knebel D, Ayali A, Guershon M, Ariel G. 2019. Intra- versus inter-group variance in collective behavior. *Sci Adv.* 5(1):eaav0695.

46 Ellis PE. 1951. The marching behaviour of hoppers of the African Migratory Locust in the laboratory *Anti-Locust Bull.* 7.

47 Fechner GT. 1860. *Elemente der psychophysik. Readings in the history of psychology.* Leipzig: Von Breitkopf und Härtel. p. 206–213.

48 Piñeiro G, Perelman S, Guerschman JP, Paruelo JM. 2008. How to evaluate models: observed vs. Predicted or predicted vs. observed? *Ecol Modell.* 216(3–4):316–322.

49 Hein AM, et al. 2020. An algorithmic approach to natural behavior. *Curr Biol.* 30(11):R663–R675.

50 McDermott JH. 2009. The cocktail party problem. *Curr Biol.* 19(22): R1024–R1027.

51 Schoepe T, et al. 2024. Finding the gap: neuromorphic motion-vision in dense environments. *Nat Commun.* 15(1):817.

52 Shen Y, Wei C. 2022. Multi-UAV flocking control with individual properties inspired by bird behavior. *Aerosp Sci Technol.* 130: 107882.

53 Bastien R, Romanczuk P. 2020. A model of collective behavior based purely on vision. *Sci Adv.* 6(6):eaay0792.

54 Buhl J, et al. 2006. From disorder to order in marching locusts. *Science.* 312(5778):1402–1406.

55 Zanon M, Potrich D, Bortot M, Vallortigara G. 2022. Towards a standardization of non-symbolic numerical experiments:

GeNEsIS, a flexible and user-friendly tool to generate controlled stimuli. *Behav Res Methods*. 54(1):146–157.

56 Leibovich T, Katzin N, Harel M, Henik A. 2017. From "sense of number" to "sense of magnitude": the role of continuous magnitudes in numerical cognition. *Behav Brain Sci*. 40:e164.

57 Serres JR, Ruffier F. 2017. Optic flow-based collision-free strategies: from insects to robots. *Arthropod Struct Dev*. 46(5):703–717.

58 Poggio T, Reichardt W. 1973. A theory of the pattern induced flight orientation of the fly Musca domestica. *Kybernetik*. 12(4):185–203.

59 Reichardt W, Wenking H. 1969. Optical detection and fixation of objects by fixed flying flies. *Naturwissenschaften*. 56(8):424–425.

60 Knebel D, Sha-Ked C, Agmon N, Ariel G, Ayali A. 2021. Collective motion as a distinct behavioral state of the individual. *iScience*. 24(4):102299.

61 Hayashi K, Locke NJM, Laudet V. 2024. Counting nemo: anemonefish Amphiprion ocellaris identify species by number of white bars. *J Exp Biol*. 227(2):jeb246357.

62 Patel RN, *et al.* 2021. Mantis shrimp identify an object by its shape rather than its color during visual recognition. *J Exp Biol*. 224(8):jeb242256.

63 Gherardi F, Cenni F, Parisi G, Aquiloni L. 2010. Visual recognition of conspecifics in the American lobster, *Homarus americanus*. *Anim Behav*. 80(4):713–719.

64 Katzir G. 1981. Visual aspects of species recognition in the damselfish *Dascyllus aruanus* L. (Pisces, Pomacentridae). *Anim Behav*. 29(3):842–849.

65 Vergara-Ovalle F, Ayala-Guerrero F, Rosas C, Sánchez-Castillo H. 2023. Novel object recognition in *Octopus maya*. *Anim Cogn*. 26(3):1065–1072.

66 Schluessel V, Fricke G, Bleckmann H. 2012. Visual discrimination and object categorization in the cichlid *Pseudotropheus* sp. *Anim Cogn*. 15(4):525–537.

67 Bengochea M, *et al.* 2023. Numerical discrimination in *Drosophila melanogaster*. *Cell Rep*. 42(7):112772.

68 Cross FR, Jackson RR. 2017. Representation of different exact numbers of prey by a spider-eating predator. *Interface Focus*. 7(3):20160035.

69 Carazo P, Fernández-Perea R, Font E. 2012. Quantity estimation based on numerical cues in the mealworm beetle (*Tenebrio molitor*). *Front Psychol*. 3:502.

70 Bortot M, *et al.* 2019. Honeybees use absolute rather than relative numerosity in number discrimination. *Biol Lett*. 15(6):20190138.

71 Bortot M, Regolin L, Vallortigara G. 2021. A sense of number in invertebrates. *Biochem Biophys Res Commun*. 564:37–42.

72 Peirce J, *et al.* 2019. Psychopy2: experiments in behavior made easy. *Behav Res Methods*. 51(1):195–203.

73 Moore RJD, *et al.* 2014. FicTrac: a visual method for tracking spherical motion and generating fictive animal paths. *J Neurosci Methods*. 225:106–119.

74 Bazazi S, Bartumeus F, Hale JJ, Couzin ID. 2012. Intermittent motion in desert locusts: behavioural complexity in simple environments. *PLoS Comput Biol*. 8(5):e1002498.